IEEE Access
Multidisciplinary ⋮ Rapid Review ⋮ Open Access Journal

Received 5 March 2022, accepted 9 June 2022, date of publication 15 June 2022, date of current version 27 June 2022.

*Digital Object Identifier 10.1109/ACCESS.2022.3183185*

# An Exemplar Pyramid Feature Extraction Based Alzheimer Disease Classification Method

**HEBA SOLIMAN ZAINA[1], SAMIR BRAHIM BELHAOUARI[1], TANYA STANKO[2], AND VLADIMIR GOROVOY[2]**

[1]College of Science and Engineering, Hamad Bin Khalifa University, Doha, Qatar
[2]Graduate School of Management, Saint Petersburgh State University, 199034 Saint Petersburgh, Russia

Corresponding author: Samir Brahim Belhaouari (sbelhaouari@hbku.edu.qa)

This work was supported by the Qatar National Library.

**ABSTRACT** Dementia is a term used to describe a variety of symptoms related to cognitive impairment in which Alzheimer disease represents 60% - 70% of the cases. As of today, there is no cure for this disease and the only way to prevent any associated medical, economic, and financial impacts or losses is to detect the disease early and work closely with suspected patients to prevent any further progress. In this research, a methodology consisting of 4 modules is proposed: (1) preprocessing, exemplar pyramid along with bi-linear interpolation followed by (2) feature extraction using Gray Level Co-Occurrence Matrix and Local Binary Pattern then (3) concatenation of all extracted features and finally (4) classification of Alzheimer disease stage using deep learning, Multi-Layer Perceptron, in particular. Our proposed method was tested using the MPRAGE structural MRI dataset from Alzheimer Disease Neuro Imaging Initiative (ADNI), and it outperformed other techniques used in the literature review. An accuracy result of 89.80 was reported for multi-class classification of 4 stages of Alzheimer disease (Cognitive Normal, Early Mild Cognitive Impairment, Late Mild Cognitive Impairment and Alzheimer Disease) for both Gray Matter (GM) and White Matter (WM). In term of binary-class classification, we were able to achieve very good results using both GM and WM. By using GM, we were able to distinguish between CN vs EMCI, EMCI vs AD and LMCI vs AD with accuracy results of 96.43%, 90.91% and 95.24% respectively. And using WM, we were able to distinguish between CN vs LMCI with 100% accuracy and EMCI vs LMCI with 95.65% accuracy. While we achieved the same accuracy result of 96.15 using both WM and GM.

**INDEX TERMS** Cognitive normal (CN), early mild cognitive impairment (EMCI), late mild cognitive impairment (LMCI), alzheimer disease (AD), local binary pattern (LBP), gray level co-occurrence matrix (GLCM), multi-layer perceptron (MLP), exemplar pyramid.

## I. INTRODUCTION

Alzheimer's disease is one of the common forms of Dementia with a possible contribution that may extent to 60% – 70% of the cases. It is considered a group of symptoms of progressive or chronic nature – in which deterioration takes place in the cognitive functions affecting the ability to process ideas or thoughts beyond what might be expected from normal ageing [1], [2]. It affects thinking, orientation, memory, learning capacity, ability to calculate, language difficulties, comprehension, and ability to judge. Controlling emotions, social activities, behavior, and motivation are commonly accompanied with an impairment in cognitive function [1], [2]. It is worth mentioning that 50 million people aged 60 and above worldwide are affected by Dementia, of which 60% lives in middle and low-income countries [1], [3], reference to the World Health Organization (WHO), it is expected that the number of people affected with Dementia will increase to reach 82 million in 2030 and 150 million in 2050 [4], [5]. This huge increase of cases will not only impact individuals' health but their families and societies. The impact may be psychological, physical, or social. In addition, there is an economic implication in terms of direct medical and social cost which was estimated in 2015 at US $818 billion [1], [6], [7].

Dementia is a progressive disease in nature; however, it depends on individual's state of health and personality, it begins with mild symptoms and ends up with sever damages in the brain. Based on symptoms, Dementia can be described

The associate editor coordinating the review of this manuscript and approving it for publication was Gangyi Jiang.


This work is licensed under a Creative Commons Attribution 4.0 License. For more information, see https://creativecommons.org/licenses/by/4.0/

in three different stages a) Early stage (first two years) b) Middle stage (2nd to 5th year) c) Late stage ($5^{th}$ year and more) [1], [2], [8]. However, researchers tend to use different terminologies while monitoring conversion of the different stages of Dementia, Alzheimer, from Healthy Controls (HC) or Cognitive Normal (CN) in early stages to Mild Cognitive Impairment (MCI) in middle stages to reach the late stage of Alzheimer (AD). In the middle stage, different acronyms are used as below:

- Mild Cognitive Impairment – Converters (MCI-C).
- Mild Cognitive Impairment – None-Converters (MCI-NC).
- Early Mild Cognitive Impairment (EMCI).
- Late Mild Cognitive Impairment (LMCI).
- Progressive Mild Cognitive Impairment (pMCI).
- Stable Mild Cognitive Impairment (sMCI).

Alzheimer disease pathophysiology is related to an injury and death of neurons in different part of the brain. This process starts in the hippocampus, which is responsible of learning and memory, then moves gradually to affect the entire brain [9], [10]. In order for a neurologist to diagnosis an individual with Alzheimer, a neurologist, after taking in consideration factors such as age, education and gender, may request a patient to make a couple of clinical tests such as Mini-Mental State Exam (MMSE), Mini-Cog Test [11] and laboratory tests such as thyroid disorder, Vitamin B-12 deficiency. In addition to biomarkers and brain imaging tests such Magnetic Resonance Imaging (MRI), Computerized Tomography and Positron Emission Tomography (PET), Fluorodeoxyglucose – Positron Emission Tomography (FDG-PET) and Cerebrospinal Fluid (CSF) [2], [11]–[13].

Due to the increased number of Alzheimer cases, its impact on individuals, societies, and economies, and since there is no cure from this disease to this date as per (WHO) [1], researchers and scientists contributed to this matter by suggesting new methodologies using Machine Learning (ML) and Deep Learning (DL) techniques. ML and DL techniques can help the neurologists in the early detection of Alzheimer's disease and prevent its progression to late stages especially with the limited availability of required and appropriately trained staff and the rapid increase of individuals with Alzheimer disease [14]–[16].

## II. BACKGROUND

In [17], a total of 287 structural MRI and its segmented WM, GM, and CSF from ADNI dataset were used along with its clinical data in order to implement multiclass classification between three stages of Alzheimer Disease (CN, MCI, and AD). In addition to the binary class classification between AD vs CN, AD vs MCI and CN vs MCI. First, [17] extracted the texture features of the structural MRI using Scale Invariant Feature Transform (SIFT), Histogram of Oriented Gradient (HOGs), Gray-Level Co-Occurrence Matrix (GLCM) and Local Binary Pattern (LBP) then applied Bag of Words (BOWs) for classification purposes. At the same time, he only applied GLCM on the segmented WM, GM, and CSF for feature extraction. The extracted features and clinical data were then input into different classifiers such as SVM, KNN, Decision Tree and Ensemble. The proposed method gave good results specially for binary class classification between AD and CN (98.9%) considering CSF However the results of the WM, GM and CSF varies between (81% - 86.7%) distinguishing between CN and MCI. Moving from texture analysis and machine learning to deep learning, [18] built a CNN model based on a single cross-sectional MRI and was able to achieve exceptionally good results diagnosing Alzheimer disease and mild cases that may convert to severe stage with time. [18] reported an accuracy result of 87.7% and 76.1 distinguishing between HC vs c-MCI and HC vs s-MCI respectively using a total of 1,409 3D T1 weighted images from ADNI-1, ADNI-2, ADNI-Go and 229 images from Milan dataset. [19] proposed a framework that consist of 361 preprocessed MRI, followed by feature extraction using Automated Anatomical Labeling (AAL) template where 90 cerebrum areas were selected and mapped to the GM images. Then, he applied Principal Component Analysis (PCA) for feature selection. Classification of Alzheimer stages was done using SVM along with the switching delayed PSO algorithm. With this proposal, [19] reported an accuracy of 76.9231% distinguishing between CN vs sMCI and 85.7143% between CN vs pMCI. In this research, [20] used 397 MRI and PET imaging datasets from ADNI along with 3D-CNN and Fully Stacked Bidirectional Long Short-Term Memory (FSBi-LSTM) to diagnose Alzheimer disease. The main idea of adding FSBi-LSTM is to extract high level spatial and semantic information and that is done by inputting 1 pixel of all the features at each step to the corresponding position. The extracted features are then fed into the SoftMax activation function for classification of the stage of the disease. An accuracy of 86.36% and 65.35% were reported distinguishing between pMCI vs CN and sMCI vs CN, respectively.

Other researchers were concerned about the binary class classification between pMCI and sMCI or what they call MCI-C vs MCI-NC. Using 1,526 subjects from ADNI-1, ADNI-2 and MIRIAD datasets, [21] was able to achieve and accuracy result of 76.9% distinguishing between pMCI vas sMCI. In his research, he proposed a framework that consist of a landmark-based deep multi-instance learning (LDMIL) for classification and Anatomical Landmarks for feature extraction. It is worth mentioning that he reported an accuracy result of 91.09% and 92.75% between AD and CN on ADNI-2 and MIRIAD datasets, respectively. The accuracy results reported by [22] were 72.2% for sMCI vs pMCI and 91.3% between CN and AD. In this study, [22] proposed multi-directional texture grading based on 3D Gabor filters such as local variance and entropy along with an innovation adaptive patch-based fusion strategy based on local confidence criterion. The experiment was implemented on a total of 800 T1 weighted MRIs from ADNI dataset. [23] was able to achieve better accuracy results of 82.75% distinguishing

between MCI-C vs MCI-NC by applying discriminative feature learning and canonical correlation analysis (CCA) on 398 subjects from both MRI and PET imagining from ADNI dataset. For feature extraction, he used the SIFT texture analysis method, which was followed by normalization, vocabulary, histogram representation, kernel mapping, then classification using SVM. This proposed method gave an accuracy result of 96.93% for the binary class classification between AD vs CN and 86.57% between MCI and CN. [24] proposed a new feature selection method by embedding the inherent of relational information into a sparse multi-task learning framework. In this study, he used 202 MRIs along with clinical data such as ADAS-Cog and MMSE from ADNI. The accuracy results reported by this experimental were 93.7% for AD vs CN, 79.7% for MCI vs CN and 71.8% for MCI-C vs MCI-NC. [25] was interested in a multi-class classification between 4 stages of Alzheimer disease (AD, LMCI, MCI, and CN). Using augmentation, he was able to increase the number of MRI subjects downloaded from ADNI dataset from 149 to 9,506, then he implemented transfer learning using three well-known CNN architectures, GoogleNet, ResNet-18 and ResNet-152. The results were 98.88%, 98.01% and 98.14, respectively.

In contrast, [26] proposed a non-linear graph fusion method for multi-class classification of three stages of Alzheimer disease (AD, MCI, and CN) using a total number of 147 subjects from different modalities from ADNI dataset such as MRI, FDG-PET, CSF bio-marker measures and categorical genetic information. 239,391 features were extracted from MRI and 239,304 features from PET, then a combination of all similarities from the different modalities were done in a non-linear graph fusion that generated a unified graph for final classification. The reported accuracy results were as follow, 60.2% for multiclass classification. 79.5% and 91.8% for binary class classification between MCI vs CN and AD vs CN. [27] proposed an ensemble of 3D densely connected convolutional networks for classification of AD, CN and MCI and was able to achieve 97.52% for multiclass classification while he reported an accuracy of 98.42 and 98.83 for binary class classification between MCI vs CN and AD vs CN respectively using a total of 833 T1 weighted MRI from ADNI dataset. In another research, [28] implemented transfer learning using CNN for the VGG-16 architecture on a total number of 150 T1 weighted structural MRIs from ADNI-1 dataset. A total number of 32 slices were selected for each subject of the 150, and that led to increase the number of images to 4,800. Using this method, [28] was able to extract 18,432 features from each image and that gave extremely good accuracy results of 95.73% for multiclass classification of CN, AD and MCI. While for binary-class classification results were reported as follow, 99.14% between AD vs CN, 99.30% between AD vs MCI and 99.22 between MCI vs CN.

## III. APPROACH

The proposed methodology consists of four modules, namely preprocessing; exemplar pyramid and bi-linear interpolation; feature extraction using Local Binary Pattern (LBP) and Gray-Level Co-Occurrence Metrix (GLCM) and feature concatenation; and finally, disease classification using Multi-Layer Perceptron (MLP). Figure 1 gives a clear overview of the proposed methodology.

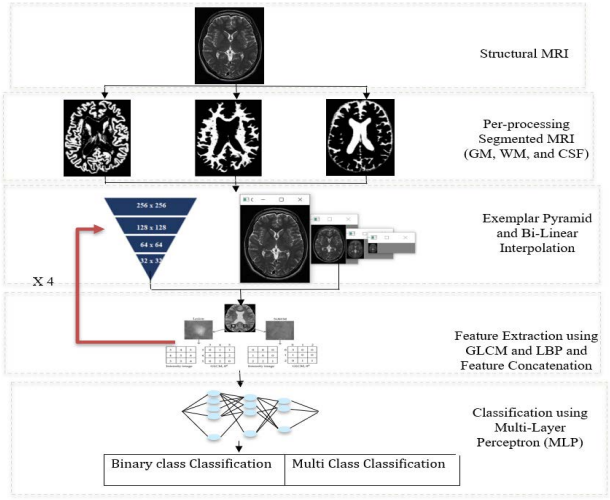


**FIGURE 1.** Proposed methodology.

### A. PRE-PROCESSING

The structural MRI in the downloaded dataset consist of Axial view of the subjects acquired using T1 weighted sequences, Figure 2 shows the segmented MRI for each classification type. The MPRAGE MRI used for training and testing were undergone the maximum preprocessing steps starting with grad-warp, B1 non-uniformity and N3 bias field correction. Grad-warp is a system specific correction of image geometry distortion due to the non-linearity of gradient. Different gradient models have different gradient non-linearity. Accordingly, the correction of image geometry enhances image information which makes the image more useful for any analysis process. B1 non-uniformity is another preprocessing step that is useful for image intensity and color correction that might be distorted due to the mishandling of radio frequency transmission. N3 bias field correction is used to correct the intensity distortion which occurs due to the dielectric effects during acquisition. [29].

In this work, we used Statistics Parametric Mapping (SPM-12) [30] along with MATLAB-R2019a [31] to segment the training and testing structural MRI into Gray Matter (GM), White Matter (WM) and Cerebrospinal fluid (CSF). This preprocessing step was performed prior the step of feature extraction.

### B. EXEMPLAR PYRAMID AND BI-LINEAR INTERPOLATION

The exemplar pyramid is a type of representation of multi-scale signal developed by different communities such as the computer vision, image processing and signal processing, in which an image or a signal is subject to repeated

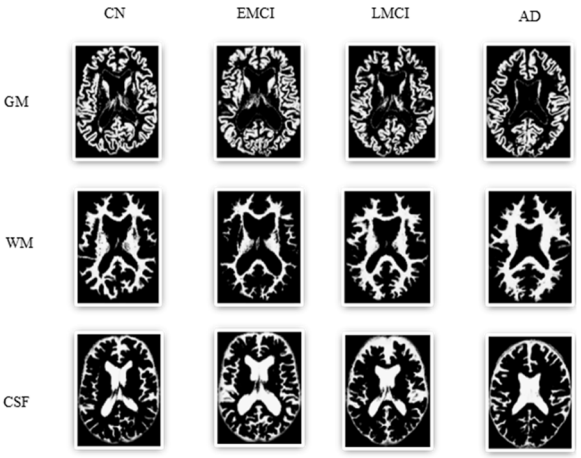


**FIGURE 2.** Sample of alzheimer disease classification classes along with the segmented MRI, GM, WM, and CSF.


**FIGURE 3.** Exemplar pyramid and bi-linear interpolation on GM image.

subsampling and smoothing [32], [33]. There are different types of exemplar pyramid such as lowpass and bandpass. In this research we conducted the lowpass exemplar pyramid which is created by smoothing the segmented MRI with a suitable smoothing filter and then subsampled the smoothed segmented MRI by a factor of 2 along the vertical and horizontal coordinate direction using bi-linear interpolation [34]. This procedure is repeated multiple times as many times as necessary in which in each cycle a smaller image with increased smoothing is produced. [35], [36]. Figure 3 shows the implementation of the exemplar pyramid and bi-linear interpolation on GM segmented image.

### C. FEATURE EXTRACTION AND CONCATONATION

In this research, we implemented two different techniques for feature extraction, however both techniques rely on texture analysis. We started by extracting features from the original segmented MRI for the WM, GM, and CSF. This was followed by downscaling the MRI using the exemplar pyramid and bi-linear interpolation and concatenation of the extracted features. This cycle was repeated for four times in which the extracted features in each cycle were concatenated all together at the end of the last cycle. This process was performed using Google Colab [37]. The below subsections clarify the texture analysis methods used for feature extraction.

### D. LOCAL BINARY PATTERN (LBP)

The LBP is used as a descriptor of shapes, motions, boundaries, and color. It gives information about objects and events.

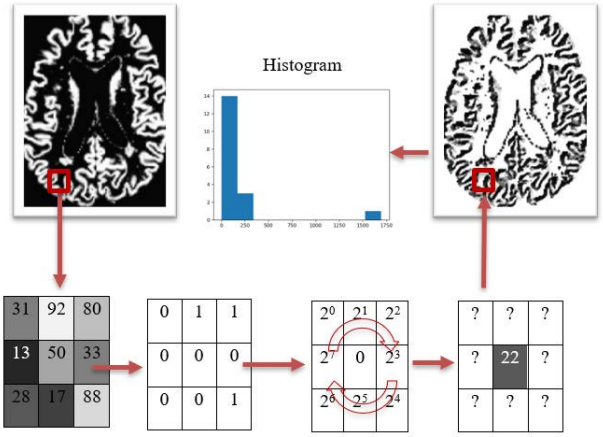


**FIGURE 4.** Computation of local binary pattern (LBP).

It is mostly used for face recognition. Also, it can be used in the medical field for noise reduction ~~recognition~~ in MRI. The main concept of LBP is to divide the image into regions or blocks, then compare the middle cell value with its surrounding neighbors. A value of 1 is given to the neighbor if its original value is greater than the middle cell value and zero otherwise. The binary digit number of the neighbors is then converted into decimal and the histogram is computed based on the frequency of each number occurring. This is followed by a normalization of histograms of all cells which gives the feature vector for the entire image [38], [39]. Figure 4 gives an overview of the computation of LBP. In this research we used Mahotas package [40] and computed the Linear Binary Pattern transform using a radius of 4 and a total number of 16 surrounding neighbors.

### E. GRAY-LEVEL CO-OCCURRENCE METRIX (GLCM)

The GLCM is an image matrix that represents the distribution of co-occurring pixel values (considering color or grayscale values) as a given offset. It computes the number of times a specific pixel value or offset occurs in an image. The GLCM was first used by Haralick back in 1973 [41] and its algorithm proposes fourteen texture based statistical features. In this research we computed only four texture features and those are entropy, contrast, correlation, and homogeneity. Figure 5 shows a general implementation of the GLCM in all possible directions [42].

The entropy measures any disorder in an image, and this means the larger the entropy, the more non-uniformity texture of that image. The contrast measures the variation in a specific area and represents the intensity transition from pixel x to pixel y separated by distance or radius r and angle $\theta$. The correlation measures the combined probability of a specified co-occurring pixel pair and the homogeneity measures how close the elements in a GLCM matrix are to its diagonal. The formulas below show how each GLCM is calculated [43], [44]

$$\text{Entropy} = \sum_{i,j=0}^{N-1} -\ln(P_{ij})P_{ij} \tag{1}$$

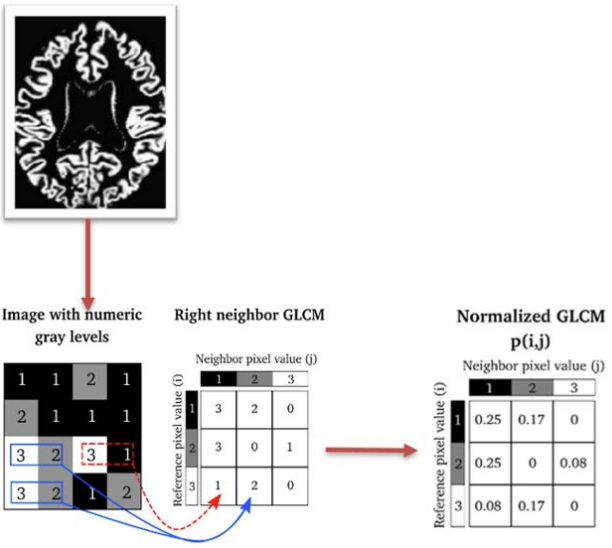


**FIGURE 5.** General implementation of GLCM.

$$\text{Contrast} = \sum_{i,j=0}^{N-1} P_{ij}(i-j)^2 \tag{2}$$

$$\text{Correlation} = \sum_{i,j=0}^{N-1} P_{ij}\frac{(i-\mu)(j-\mu)}{\sigma^2} \tag{3}$$

$$\text{Homogeneity} = \sum_{i,j=0}^{N-1} -\text{in}(P_{ij})P_{ij} \tag{4}$$

In this research, the implementation of the 4 GLCM explained above was done by calculating the radius or distance of three points away from the pixel of interest along with 4 different directions or angles (0°, 45°, 90° and 135°) resulting a total number of 37 extracted features per image size which is equal to 148 extracted features per image for each segmented MRI.

## IV. DISEASE CLASSIFCATION

The last step of the proposed methodology is classifying the stage of Alzheimer disease using Deep Learning and in particular, Multi-Layer Perceptron [43], [45], [46]. In this research we have implemented a multiclass classification between four different stages and those are the Cognitive Normal (CN), Early Mild Cognitive Impairment (EMCI), Late Mild Cognitive Impairment (LMCI) and Alzheimer stage (AD). In addition to that, we have done a binary class classification to distinguish between the different stages for the three segmented MRI.

The Deep Learning used in this research consist of an input layer with all extracted features, followed by three hidden layers and an output classification layer. The first hidden layer consists of 6,000 neurons, followed by second hidden layer with 5,000 neuron and a third hidden layer with 4,000 neurons. The input layer along with the three hidden layers were activated using Relu activation function. The output layer consists of 4 neurons in case of multiclass classification and was activated using SoftMax activation function. Figure 6 shows the overall architecture of the Multi-Layer Perceptron (MLP) for the multi-class classification.

On the other hand, the output of the binary-class classification is represented by only 1 neuron and activated using Sigmoid activation function. Figure 7 shows an overall architecture of the binary-class classification. Both models (Multiclass and binary-class classification) were fine-tuned using normal distribution kernel initializer and each layer was followed by a dropout in order to remove 10% of the unnecessary weights. The weights were updated using Adam optimizer which is considered a stochastic gradient descent method that is based on adaptive estimation of first order and second-order moments.

## V. DISCUSSION

The below subsections present the details of the dataset used along with the results achieved after conducting the experimental during this study.

### A. DATASET

The dataset used in this research was obtained from the Alzheimer's Disease Neuroimaging Initiative (ADNI) which provides researchers with subjects of different datatypes such as MRI, PET images, genetics, cognitive tests, clinical data, CSF, and blood biomarkers that may help in predicting Alzheimer's disease and its progress over time. In this study, we downloaded a total of 311 preprocessed T1 weighted structural MRI obtained by 3 Tesla Philips Medical System with a thickness of 1.2mm and flip angle of 9° and a (256, 256,170) matrix. This dataset is recommended by ADNI and is given the name MPRAGE, it has undergone the maximum preprocessing steps starting with grad-warp followed by B1 non-uniformity and N3. [29].

In this study, we targeted elderly people from both sexes, male and female, within the range of 75-95 years old in which the dataset used in this experiment consists of 106 subjects representing CN, 83 EMCI, 65 LMCI and 57 for AD. These Structural MRI were then segmented into GM, WM and CSF using SPM-12 App [30] along with MATLAB-R2019a [31]. An axial view of the middle slice, slice number 28, was chosen from the range [−57.7] - [85.6] of the available slices to extract features and do the classification accordingly. The dataset was then divided into training and testing where 80% represented the training and 20% represented the testing. Table 1 gives a brief description about the subjects chosen in this study.

### B. CLASSIFICATION AND RESULTS

In this study, features were extracted by analyzing the texture of the original image and its subsamples after applying the exemplar pyramid technique and bi-linear interpolation for 3 times. All extracted features were then concatenated to represent the texture of 4 GLCM such as entropy, contrast, correlation, and homogeneity. In addition to the texture of the LBP. A total number of 109,628 features were reported

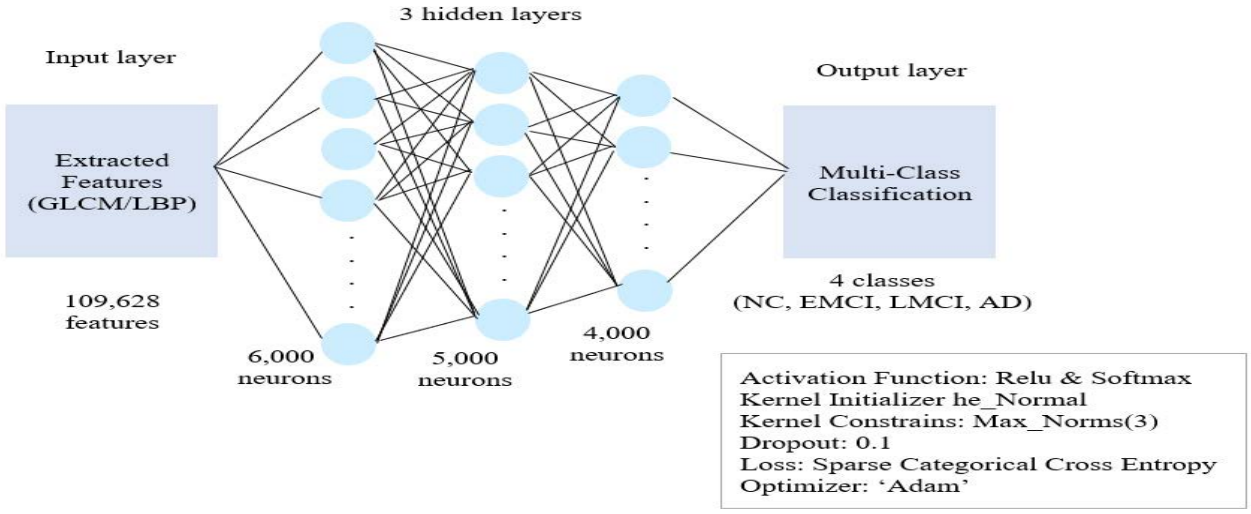


**FIGURE 6.** Multi-layer perceptron (MLP) – multiclass classification.

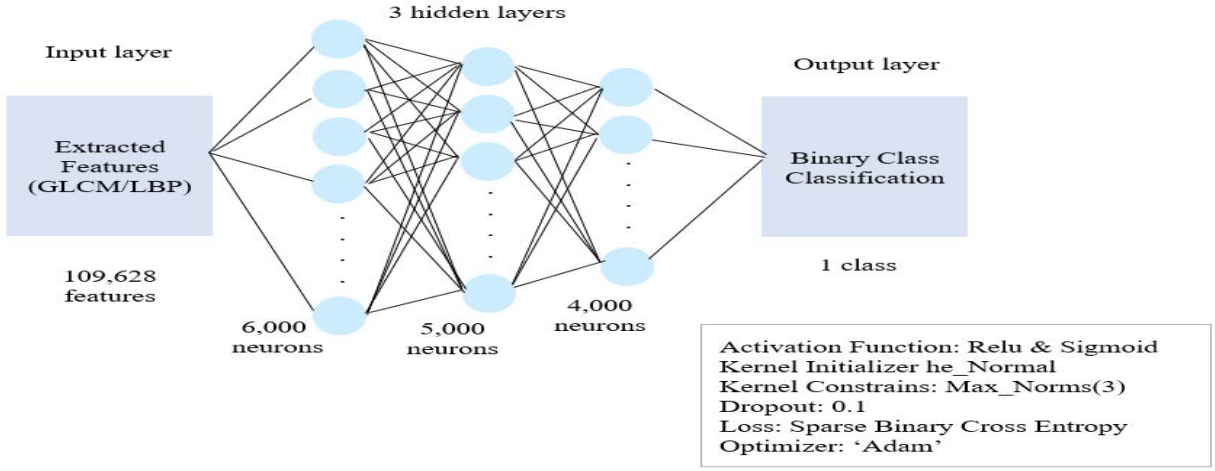


**FIGURE 7.** Multi-layer perceptron (MLP) – binary-class classification.

**TABLE 1.** Distribution of subjects among female and male.

| Class | AD | | CN | | EMCI | | LMCI | |
|---|---|---|---|---|---|---|---|---|
| Age | F | M | F | M | F | M | F | M |
| [75-80] | 14 | 18 | 37 | 12 | 16 | 38 | 19 | 22 |
| 80-85] | 9 | 11 | 15 | 24 | 19 | 4 | 9 | 2 |
| [85-90] | 5 | - | 4 | 13 | 1 | 3 | 4 | 9 |
| [90-95] | - | - | 1 | - | - | 2 | - | - |
| Total | 57 | | 106 | | 83 | | 65 | |

in this experiment. A multi-Layer Perceptron was then used for classification purposes. Three different approaches were used for classification and explained below.

### C. MULTICLASS CLASSIFICATION

We implemented a multi-class classification using Deep Learning, multi-layer perceptron. The deep learning consists of an input layer with all extracted features followed by three hidden layers and an output layer of 4 classes. The three hidden layers contains (6,000, 5,000 and 4,000) neurons, respectively. We used the dropout layer between all layers in this deep learning in order to remove 10% of the unnecessary weights and make the algorithm more efficient. Relu activation function was used in all layers except the output layer which was activated using SoftMax and Adam was used as an optimizer. We have implemented the experiment using GM, WM and CSF and reported the results accordingly. Table 2 shows that both GM and WM achieved the same accuracy results of 89.80% while the CSF reported less accurate results of 83.67%.

### D. BINARY-CLASS CLASSIFICATION

We also implemented a binary-class classification using Deep Learning, multi-layer perceptron. This deep learning consists of an input layer with all extracted features followed by three hidden layers and an output layer of 1 class. The three hidden

**TABLE 2.** Multiclass classification and binary class classification results using MLP.

| | Train | Test | CSF | GM | WM |
|---|---|---|---|---|---|
| Multiclass | 262 | 49 | 0.8367 | 0.8980 | 0.8980 |
| CN vs EMCI | 161 | 28 | 0.8929 | 0.9643 | 0.9286 |
| CN vs LMCI | 144 | 27 | 0.8148 | 0.9630 | 1.0 |
| CN vs AD | 137 | 26 | 0.9231 | 0.9615 | 0.9615 |
| EMCI vs LMCI | 125 | 23 | 0.8696 | 0.8696 | 0.9565 |
| EMCI vs AD | 118 | 22 | 0.7727 | 0.9091 | 0.8636 |
| LMCI vs AD | 101 | 21 | 0.9524 | 0.9524 | 0.9048 |

**TABLE 3.** Accuracy results by combining segmented images and using transfer learning.

| | Training | Testing | Accuracy results |
|---|---|---|---|
| GM+WM+CSF | 786 | 147 | 0.6122 |
| GM+WM | 524 | 98 | 0.7857 |
| Transfer Learning using GM+WM | 524 | 98 | 0.6531 |

**TABLE 4.** Comparison between our proposed method and [17] from a texture analysis perspective on segmented CSF, GM, WM, and combination of three of them.

| Approach | Modality | CSF | GM | WM | GM+WM+CSF |
|---|---|---|---|---|---|
| [17] | MRI | 78.6% | 71.4% | 77.0% | 61.3% |
| Proposed method | MRI | 83.6% | 89.8% | 89.8% | 61.2% |

**TABLE 5.** Comparison between our proposed method and literature review accuracy results using segmented GM and ADNI dataset.

| Approach | Modality | Multiclass | CN vs EMCI | CN vs LMCI | CN vs AD | EMCI vs LMCI | EMCI vs AD | LMCI vs AD |
|---|---|---|---|---|---|---|---|---|
| [18] | MRI | — | 76.1% | 87.1% | 99.2% | 75.1% | 85.9% | 75.4% |
| [19] | MRI | — | 76.92% | 85.71% | 81.25% | 69.23% | 71.23% | 57.14% |
| [20] | MRI+PET | — | 65.35% | 86.36% | 94.82% | — | — | — |
| [21] | MRI | — | — | — | 91.09% | 76.90% | — | — |
| [22] | MRI | — | — | — | 91.3% | 72.2% | — | — |
| [23] | MRI+PET | — | — | — | 96.93% | 82.75% | — | — |
| [24] | MRI | — | — | — | 93.7% | 71.8% | — | — |
| [25] | MRI | 3 classes | — | — | — | — | — | — |
| Our Method | MRI | 4 classes | 96.42% | 96.30% | 96.15% | 86.96% | 90.91% | 95.24% |

layers contain (6,000, 5,000 and 4,000) neurons, respectively. We used the dropout layer between all layers in this deep learning to remove 10% of the un-necessary weights and make the algorithm more efficient. The Relu activation function was used in all layers except the output layer which was activated using Sigmoid and Adam was used as an optimizer. We have implemented the experiment using GM, WM and CSF and reported the results accordingly between CN vs EMCI, LMCI and AD. EMCI vs LMCI and AD and LMCI and AD.

Table 2 gives an overview of the results achieved using binary-class classification, in which the WM surpass GM with accuracy results 100% and 95.65% distinguishing between CN vs LMCI and EMCI vs LMCI, respectively. In contrast, GM surpass WM distinguishing between EMCI vs AD with accuracy of 90.91% and 95.24% between LMCI vs AD. The same accuracy results were achieved for GM and WM distinguishing between CN vs AD. Most of the results reported using the segmented CSF were less accurate than those reported using GM and WM. These results are promising when talking about detecting Alzheimer in an early stage and preventing further progress and associated financial, medical, economic and societal losses.

### E. COMBINING SEGMENTED MRI IMAGING

We combined the segmented images from the structure MRI, implemented the same methodology for multi-class classification and reported the results accordingly. In the first experiment, we combined GM, WM, and CSF images and started the training process and in the second experiment we combined only GM and WM images since we achieved particularly good results using both separately. Table 3 gives an overview of the results achieved.

### F. TRANSFER LEARNING RESULTS (GM AND WM)

In another experiment, we tried to apply transfer learning between the segmented images (GM and WM) since the

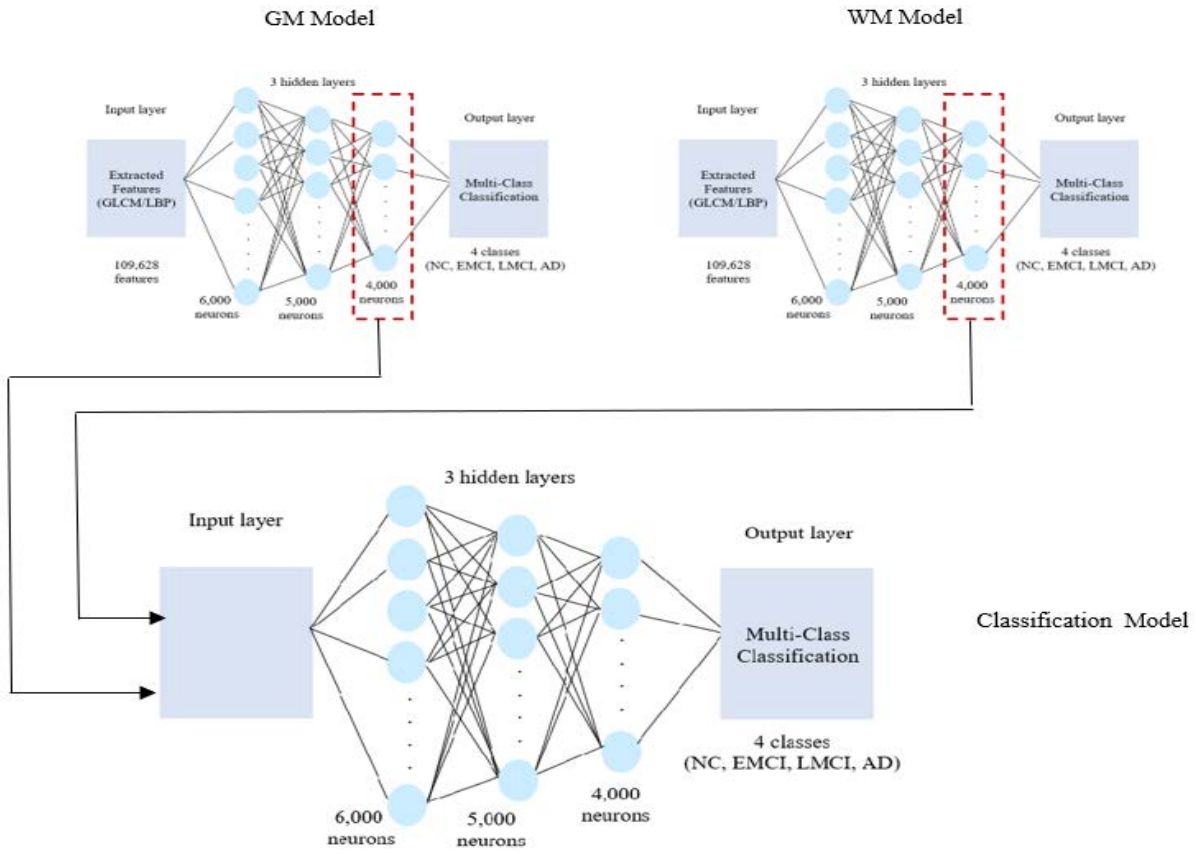


**FIGURE 8.** Transfer learning between WM and GM.

overall reported results were promising for each one separately in which the performance of the GM surpasses the performance of the WM in some cases and vice versa in other cases. Figure 8 gives an overview of the overall structure of the transfer learning implementation.

Using transfer learning, we created a new model in which the input represented from the last layer of the Gray Matter model and the last layer of the White Matter model. The model consists of three hidden layers and represented by (6,000, 5,000 and 4,000) neurons, respectively. We used the dropout layer between all layers in this deep learning in order to remove 10% of the un-necessary weights and make the algorithm more efficient. Relu activation function was used in all layers except the output layer which was activated using SoftMax and Adam was used as an optimizer.

Table 3 shows the results of combining GM, WM, and CSF, the combination between GM and WM and the accuracy results of transfer learning between GM and WM.

## VI. PROPOSED METHOD AND LITRATURE REVIEW RESULTS

In comparison between our proposed methodology and the results achieved from the literature review, table 4 shows that our proposed method performs better than those results achieved by [17] in GM, WM, and CSF. However, our proposed method gave almost the same results achieved by [17] when combining GM, WM, and CSF with a ridiculously small difference.

From another perspective, table 5 shows that our proposed method exceeds the results of those in the literature review, especially in the binary class classification considering only the GM. We were able to achieve particularly good results distinguishing between CN vs EMCI, CN vs LMCI, EMCI vs LMCI, EMCI vs AD and LMCI vs AD. However, the proposed method by [18] reported better accuracy than those we achieved distinguishing between CN vs AD with a slight difference of 3.05%. Most of the literature reviews were concerned about the 3 stages (CN, MCI, and AD) of Alzheimer's disease such as [25] who was able to achieve an accuracy result of 98.88%.

## VII. RESEARCH FINDINGS

In this research, we implemented the exemplar pyramid technique along with bi-linear interpolation for the segmented MRI and its subsamples. From this experiment, we found out that downscaling the original image up to 3 times gave us the best results in terms of accuracy, recall, and specificity. The GLCM and LBP texture analysis used in this study helped in the process of detecting Alzheimer's disease in its early stage with high accuracy results for both GM and

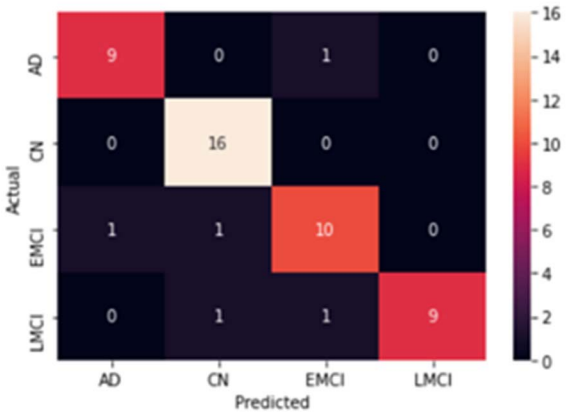


**FIGURE 9.** Confusion matrix for multiclass classification using Gray Matter (GM).

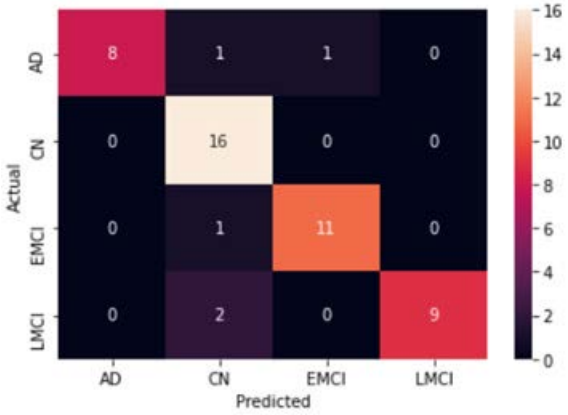


**FIGURE 10.** Confusion matrix for multiclass classification using White Matter (WM).

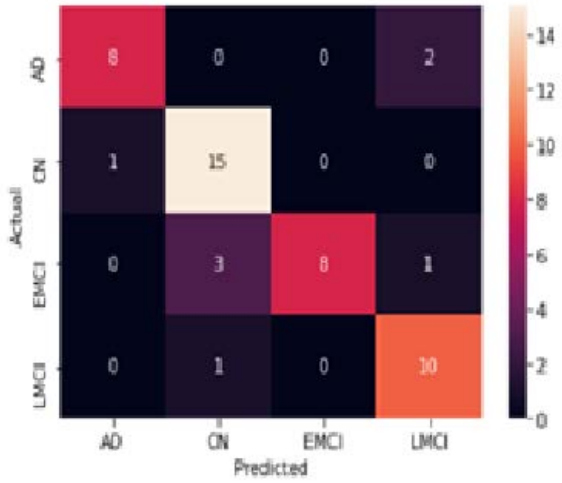


**FIGURE 11.** Confusion matrix for multiclass classification using Cerebrospinal Fluid (CSF).

WM. In general, we can say that GM and WM give the same accuracy results in terms of multi-class classification. The GM gives better results in terms of binary class classification distinguishing between the CN and EMCI, however the WM gives better results in terms of distinguishing between the CN and LMCI. Both GM and WM give the same accuracy results distinguishing between the CN and AD.

Combining the segmented images from the structural MRI did not give better results than those achieved using each individual segmented image separately. Also, the reported results from transfer learning between the GM and the WM did not meet our expectations.

In the future, we can apply the same methodology considering additional datatypes such as PET images, genetics, clinical data, cognitive tests, and blood biomarkers in order to provide higher accuracy results and better classification of Alzheimer's disease and its different stages.

## VIII. CONCLUSION

In this paper, we proposed an exemplar pyramid technique along with bi-linear interpolation in which the MRI images were downscaled for 3 times. Using this technique, we were able to extract different features using Local Binary Pattern and four texture features using Gray Level Co-Occurrence Matrix (Entropy, Contrast, Correlation and Homogeneity).

The extracted features were concatenated, and a multi-layer perceptron was used for classification. We applied two different classification techniques, multi-class classification between 4 categories, CN, EMCI, LMCI and AD and a binary class classification.

Using a dataset from ADNI, we segmented the MRI into Gray Matter, White Matter and CSF and applied our proposed methodology and reported the results accordingly. We reported high accuracy results in term of binary class classification for the GM distinguishing between CN and EMCI and high accuracy results for the WM distinguishing between CN and LMCI and same results for both GM and WM distinguishing between CN and AD. The results are promising and can be used to detect Alzheimer disease effectively and efficiently in an early stage and prevent its progress and any associated losses.

## IX. CONFUSION MATRIX FOR MULTI-CLASS CLASSIFICATION

Using Gray Matter (GM), See Fig. 9.
Using White Matter (WM), See Fig. 10.
Using CSF, See Fig. 11.

## ACKNOWLEDGMENT

The authors would like to thank ADNI for providing them with access to the dataset and for supporting their research and for approving it for publication.

## REFERENCES

[1] WHO. (2021). *Dementia*. [Online]. Available: https://www.who.int/news-room/fact-sheets/detail/dementia.
[2] (2021). *Alzheimer's Disease Fact Sheet*. [Online]. Available: https://www.nia.nih.gov/health/alzheimers-disease-fact-sheet.
[3] MayoClinic. (2021). *Alzheimer's Disease*. [Online]. Available: https://www.mayoclinic.org/diseases-conditions/alzheimers-disease/symptoms-causes/syc-20350447

[4] *Risk Reduction of Cognitive Decline and Dementia: WHO Guidelines*, World Health Organization, Geneva, Switzerland, 2019.
[5] A. Rosenberg, F. Mangialasche, T. Ngandu, A. Solomon, and M. Kivipelto, "Multidomain interventions to prevent cognitive impairment, Alzheimer's disease, and dementia: From FINGER to world-wide FINGERS," *J. Prevention Alzheimer's Disease*, vol. 7, no. 1, pp. 29–36, 2020.
[6] M. Sado, A. Ninomiya, R. Shikimoto, B. Ikeda, T. Baba, K. Yoshimura, and M. Mimura, "The estimated cost of dementia in japan, the most aged society in the world," *PLoS ONE*, vol. 13, no. 11, Nov. 2018, Art. no. e0206508.
[7] A. Adlimoghaddam, B. Roy, and B. C. Albensi, "Future trends and the economic burden of dementia in manitoba: Comparison with the rest of Canada and the world," *Neuroepidemiology*, vol. 51, nos. 1–2, pp. 71–81, 2018.
[8] T. Ahonen and M. Pietikäinen, "Soft histograms for local binary patterns," in *Proc. Finnish signal Process. Symp. (FINSIG)*, vol. 5, 2007, p. 1.
[9] D. Bredesen, *The End of Alzheimer's: The First Program to Prevent and Reverse Cognitive Decline*. Baltimore, MD, USA: Penguin, 2017.
[10] P. M. Doraiswamy, L. P. Gwyther, and T. Adler, *The Alzheimer's Action Plan: The Experts' Guide to the Best Diagnosis and Treatment for Memory Problems*. New York, NY, USA: Macmillan, 2008.
[11] ASC (2021). *Medical Tests for Diagnosing Alzheimer's*. [Online]. Available: https://www.alz.org/alzheimers-dementia/diagnosis/medical_tests
[12] L. F. Scinto and K. R. Daffner, *Early Diagnosis of Alzheimer's Disease*. Springer, 2000.
[13] M. M. Shores, P. Ryan-Dykes, R. M. Williams, B. Mamerto, T. Sadak, M. Pascualy, B. L. Felker, M. Zweigle, P. Nichol, and E. R. Peskind, "Identifying undiagnosed dementia in residential care veterans: Comparing telemedicine to in-person clinical examination," *Int. J. Geriatric Psychiatry*, vol. 19, no. 2, pp. 101–108, Feb. 2004.
[14] D. Ravi, C. Wong, and F. Deligianni, "Deep learning for health informatics," *IEEE J. Biomed. Health Inform.*, vol. 21, no. 1, pp. 4–21, Jan. 2017.
[15] T. Ching, D. S. Himmelstein, and B. K. Beaulieu-Jones, "Opportunities and obstacles for deep learning in biology and medicine," *J. Roy. Soc. Interface*, vol. 15, no. 141, 2018, Art. no. 20170387.
[16] I. Goodfellow, Y. Bengio, and A. Courville, *Deep Learning*. Cambridge, MA, USA: MIT Press, 2016.
[17] T. Altaf, S. M. Anwar, N. Gul, M. N. Majeed, and M. Majid, "Multi-class Alzheimer's disease classification using image and clinical features," *Biomed. Signal Process. Control*, vol. 43, pp. 64–74, May 2018.
[18] S. Basaia, F. Agosta, L. Wagner, E. Canu, G. Magnani, R. Santangelo, and M. Filippi, "Automated classification of Alzheimer's disease and mild cognitive impairment using a single MRI and deep neural networks," *NeuroImage: Clin.*, vol. 21, 2019, Art. no. 101645.
[19] N. Zeng, H. Qiu, Z. Wang, W. Liu, H. Zhang, and Y. Li, "A new switching-delayed-PSO-based optimized SVM algorithm for diagnosis of Alzheimer's disease," *Neurocomputing*, vol. 320, pp. 195–202, Oct. 2018.
[20] C. Feng, A. Elazab, P. Yang, T. Wang, F. Zhou, H. Hu, X. Xiao, and B. Lei, "Deep learning framework for Alzheimer's disease diagnosis via 3D-CNN and FSBi-LSTM," *IEEE Access*, vol. 7, pp. 63605–63618, 2019.
[21] M. Liu, J. Zhang, E. Adeli, and D. Shen, "Landmark-based deep multi-instance learning for brain disease diagnosis," *Med. Image Anal.*, vol. 43, pp. 157–168, Jan. 2018.
[22] K. Hett, V.-T. Ta, J. V. Manjón, and P. Coupé, "Adaptive fusion of texture-based grading for Alzheimer's disease classification," *Computerized Med. Imag. Graph.*, vol. 70, pp. 8–16, Dec. 2018.
[23] B. Lei, S. Chen, D. Ni, and T. Wang, "Discriminative learning for Alzheimer's disease diagnosis via canonical correlation analysis and multimodal fusion," *Frontiers Aging Neurosci.*, vol. 8, p. 77, May 2016.
[24] X. Zhu, H. I. Suk, L. Wang, S. W. Lee, and D. Shen, "A novel relational regularization feature selection method for joint regression and classification in ad diagnosis," *Med. Image Anal.*, vol. 38, pp. 205–214, Apr. 2017.
[25] A. Farooq, S. Anwar, M. Awais, and S. Rehman, "A deep CNN based multi-class classification of Alzheimer's disease using MRI," in *Proc. IEEE Int. Conf. Imag. Syst. Techn. (IST)*, Oct. 2017, pp. 1–6.
[26] T. Tong, K. Gray, Q. Gao, L. Chen, and D. Rueckert, "Multi-modal classification of Alzheimer's disease using nonlinear graph fusion," *Pattern Recognit.*, vol. 63, pp. 171–181, Mar. 2017.
[27] H. Wang, Y. Shen, S. Wang, T. Xiao, L. Deng, and X. Wang, "Ensemble of 3D densely connected convolutional network for diagnosis of mild cognitive impairment and Alzheimer's disease," *Neurocomputing*, vol. 333, pp. 145–156, Mar. 2019.
[28] R. Jain, N. Jain, A. Aggarwal, and D. J. Hemanth, "Convolutional neural network based Alzheimer's disease classification from magnetic resonance brain images," *Cogn. Syst. Res.*, vol. 57, pp. 147–159, Oct. 2019.
[29] ADNI. (2017). *Mri Acquisition*. [Online]. Available: http://adni.loni.usc.edu/methods/mri-tool/mri-analysis/
[30] SPM. (1991). *Statistical Parametric Mapping*. [Online]. Available: https://www.fil.ion.ucl.ac.U.K./spm/
[31] MATLAB. (1994). *Mathworks*. [Online]. Available: https://www.mathworks.com/downloads/
[32] H. Li, Z. Lin, J. Brandt, X. Shen, and G. Hua, "Efficient boosted exemplar-based face detection," in *Proc. IEEE Conf. Comput. Vis. Pattern Recognit.*, Jun. 2014, pp. 1843–1850.
[33] F. Ozyurt, T. Tuncer, and A. Subasi, "An automated COVID-19 detection based on fused dynamic exemplar pyramid feature extraction and hybrid feature selection using deep learning," *Comput. Biol. Med.*, vol. 132, May 2021, Art. no. 104356.
[34] P. Monasse, "Extraction of the level lines of a bilinear image," *Image Process. Line*, vol. 9, pp. 205–219, Aug. 2019.
[35] GoogleColab. (2010). *Welcome to Colaboratory*. [Online]. Available: https: //colab.research.google.com/notebooks/intro.ipynb
[36] Mayo. (2021). *Alzheimer's Disease Research Center*. [Online]. Available: https://www.mayo.edu/research/centers-programs/alzheimersdisease-research-center/about
[37] Mahotas. (2016). *Local Binary Patterns*. [Online]. Available: https://mahotas.readthedocs.io/en/latest/lbp.html
[38] R. M. Haralick, K. Shanmugam, and I. Dinstein, "Textural features for image classification," *IEEE Trans. Syst., Man, Cybern.*, vol. SMC-3, no. 6, pp. 610–621, Nov. 1973.
[39] Y. Cai, G. Xu, A. Li, and X. Wang, "A novel improved local binary pattern and its application to the fault diagnosis of diesel engine," *Shock Vibrat.*, vol. 2020, pp. 1–15, Feb. 2020.
[40] C. M. Bishop, *Neural Networks for Pattern Recognition*. Oxford, U.K.: Oxford Univ. Press, 1995.
[41] K. P. S. Shijin, "Extraction of texture features using GLCM and shape features using connected regions," *Int. J. Eng. Technol.*, vol. 8, no. 6, pp. 2926–2930, Dec. 2016.
[42] A. Ali, S. Qadri, W. K. Mashwani, S. Brahim Belhaouari, S. Naeem, S. Rafique, F. Jamal, C. Chesneau, and S. Anam, "Machine learning approach for the classification of corn seed using hybrid features," *Int. J. Food Properties*, vol. 23, no. 1, pp. 1110–1124, Jan. 2020.
[43] S. Demir, S. Key, T. Tuncer, and S. Dogan, "An exemplar pyramid feature extraction based humerus fracture classification method," *Med. Hypotheses*, vol. 140, Jul. 2020, Art. no. 109663.
[44] S. Jafarpour, Z. Sedghi, and M. C. Amirani, "A robust brain MRI classification with GLCM features," *Int. J. Comput. Appl.*, vol. 37, no. 12, pp. 1–5, 2012.
[45] H. Taud and J. Mas, "Multilayer perceptron (MLP)," in *Geomatic Approaches for Modeling Land Change Scenarios*. Springer, 2018, pp. 451–455.
[46] S.-H. Wang, Y. Zhang, Y. J. Li, W. J. Jia, and F. Y. Liu, "Single slice based detection for Alzheimer's disease via wavelet entropy and multilayer perceptron trained by biogeography-based optimization," *Multimedia Tools Appl.*, vol. 77, no. 9, pp. 10393–10417, 2018.

**HEBA SOLIMAN ZAINA** received the bachelor's degree in computer science from the Arab Academy for Science and Technology and Maritime Transport, Doha, Qatar, in 2003, and the M.S. degree in data science and engineering from Hamad Bin Khalifa University (HBKU), Doha, in 2021. Since 2012, she has been a Senior Quality of Service Researcher with the Communications Regulatory Authority, Doha. Her research interests include data analysis, image processing, artificial intelligence, and deep learning.

**SAMIR BRAHIM BELHAOUARI** received the master's degree in telecommunications and network from the Institute National Polytechnique of Toulouse, France, in 2000, and the Ph.D. degree in mathematics from the Federal Polytechnic School of Lausanne-Switzerland, in 2006. He is currently an Associate Professor with the Division of Information and Communication Technologies, College of Science and Engineering, University of Hamad Bin Khalifa, Qatar Foundation. During the last years, he also holds several research and teaching positions at Innopolis University, Russia; AL Faisal University, Saudi Arabia; the University of Sharjah, UAE; University Technology PETRONAS, Malaysia; and the EPFL Federal Swiss School, Switzerland. His research interests include applied mathematics, statistics, and data analysis until artificial intelligence, image, and signal processing (biomedical, bioinformatics, forecasting, etc.), since he is from mathematics and computer science background.

**TANYA STANKO** received the bachelor's and master's degrees in applied mathematics from the Moscow Institute of Physics and Technology, Russia, in 2004, and the Ph.D. degree in computational fluid dynamics from the University of Leeds, U.K., in 2011. She was an experienced Researcher at the Department of Engineering, Technical University of Munich, Germany. Since 2012, she has been in leadership positions with various universities in Russia. Her research interests include engineering education and quantitative tools for data analysis.

**VLADIMIR GOROVOY** received the graduate degree from the Mathematics and Mechanics Department, Saint Petersburg State University, Russia, in 2004, and the Ph.D. degree in computer science from Saint Petersburg State Polytechnical University, in 2012. Since then, he has been a Lecturer with the Saint Petersburg State University and a Developer, a Team Leader, the Head of Service, and a Product Manager with Tech Giant Yandex. His research interests include data mining, deep learning, knowledge management, and ontological engineering.